

# Digital Wide-Area Survey from Aerial Photographs

Sam Redfern

I.T. Dept. & Dept. of Archaeology  
NUI, Galway,  
Ireland.  
sam.redfern@nuigalway.ie

**Abstract.** This paper discusses the development and testing of digital image processing, mapping, and classification techniques applied to the various tasks of computer-assisted aerial archaeology. These techniques are presented specifically in the context of the Aerial Archaeology System (AAS) – a software package proposed as an integral component of the archaeologist's geographical information system (GIS) toolset. The AAS was described in an earlier CAA paper (Redfern 1999a); the emphasis of the current paper is therefore on the developments made in the last 2 years, which include the development of a classification system and the scientific testing of other aspects of the AAS.

**Keywords:** Digital image techniques, aerial photography.

## 1 Introduction

Aerial photography, which has been used by archaeologists since Crawford's pioneering work in the 1920s (Crawford 1929), is today the single most important technique for the initial discovery of archaeological sites, and is also one of the most important for their recording and subsequent analysis (Darvill 1996). In recent times, as the number of excavations carried out has decreased, the need for non-invasive analytical techniques has become greater. The importance of aerial photography today is greater than ever, as an increasing proportion of archaeological assessment is geared towards prioritising the importance of sites for preservation in the current climate of accelerating rural development (Hampton 1983; Hingley 1991).

Despite the fact that archives of aerial photographs are available for many regions, there is generally a lack of available time and resources to adequately study this rich source of archaeological information by traditional methods (Riley 1987; Palmer 1991). The digital tools of image processing, photogrammetry, and pattern recognition have the potential to improve the efficiency and objectivity of aerial archaeology, and some developments have been made to this end.

The applications of computers to aerial archaeology falls into three categories:

- **Automatic or assisted identification and mapping of archaeological sites.** Image enhancement techniques have been successfully used for a number of years for assisting the manual study of low contrast archaeological material in aerial photographs (Scollar 1990), and recently attempts have also been made to *automate* the process of monument discovery and mapping (Lemmens *et al.* 1993; Redfern 1997, 1999a).
- **Geometric rectification and photogrammetry.** The geometric correction of distorted oblique aerial photographs is perhaps the most established computer application in aerial archaeology (e.g. Haigh *et al.* 1983; Scollar 1990). A related technology that has emerged only recently as a desktop computer

application is topographic photogrammetry, whereby stereo pairs of photos are used to generate digital elevation models (DEM) of the imaged landscape.

- **Higher-level assistance with site interpretation.** The technique of numerical, morphology-based typological classification has been recently applied to archaeological monuments in order to establish new classification schemes. Structured description (Edis *et al.* 1989) and automated pattern recognition (Redfern *et al.* 1998) have been used to assign newly discovered monuments to typological classes. GIS-based analyses, in which additional archaeological and environmental data is leveraged, also have an essential role in site interpretation.

The Aerial Archaeology System (AAS) is a *Windows* software package that provides a variety of digital tools for use by archaeologists studying stereo pairs of vertical photographs. The software provides assistance in each of the three areas outlined above. The basic techniques underlying the extraction and measurement of monuments have been dealt with previously (Redfern 1997), as has a detailed description of the AAS itself (Redfern 1999a), though in summary the main features are:

- Calculation of scale, location, and orientation of photographs based on user-supplied control points;
- Assisted discovery and accurate tracing of archaeological features in the photographs;
- Automatic morphological measurement of these features, and calculation of their location in the user's co-ordinate system;
- Creation of DEMs of monuments and their immediate localities through analysis of overlapping stereo pairs of photographs;
- Integrated database management of all primary and derived data in the system;
- Export of data products in common formats;
- Automated assignment of monuments to typological classes, through analysis of morphological and to-

pographic descriptors, in order to assist their initial interpretation as they are discovered.

Archaeological survey is often approached using a hierarchical strategy, beginning with a general appraisal of a relatively wide area, and using this to inform the selection of smaller and smaller regions, which are studied in greater and greater detail. It is intended that the AAS contributes to the initial stages of such a strategy, which is where medium altitude aerial photographs typically have a role to play. The rapid and objective collection of as much archaeological information as is available in stereo aerial photographs is facilitated. It is important to recognise that objectivity is a key concern as archaeological monument databases cover increasingly large areas: without consistency among the data produced by the many contributing users, database queries cannot be usefully applied.

The current paper, in describing the developments made in the last two years, emphasises the scientific testing of the monument extraction and photogrammetry systems, and the development and implementation of the classification system. It also describes aspects of an analytical GIS-based study of an archaeological landscape, which was contributed to by the AAS, and which provides a basis for assessing the AAS and making recommendations for future developments.

## 2 Monument Detection and Mapping

### 2.1 The Monument Mapping Technique

The automatic detection and mapping of archaeological evidence from aerial photographs poses significant challenges for digital image processing. The major sources of these difficulties are:

1. the extremely low signal-to-noise ratio of most monuments visible in aerial photographs;
2. the fact that earthwork monument boundaries do not adhere to any strict morphological constraints, other than the fact that many can be loosely defined as 'sub-circular' closed loops;
3. the fact that nearly all monuments are visible only as thin boundary features, with no morphologically or texturally recognisable internal features;
4. the presence of clutter – primarily modern day objects of relatively high contrast, such as walls, houses, trees, and roads;
5. monument damage and occlusion, both of which further add to the problem of incomplete boundary evidence.

Template-based pattern recognition techniques such as the Hough Transform, when looking for circular shapes, essentially sum the number of 'edge' pixels<sup>1</sup> at a given

distance from a point, thereby examining evidence for the existence of a circle centred at that point (Hough 1962). Clearly, archaeological monuments are rarely perfect circles: the AAS software therefore identifies and aggregates many small arcs from circles with varying radii and centre points. The steps outlined below are carried out in this procedure, which is described in more detail in (Redfern *et al.* 1998):

1. An approximate area (rectangle) containing the shape is identified, either by the user or by another image processing algorithm. It is assumed that a small region around the centre of this area contains all candidate arc centres, and that their potential radii fall within 25% and 50% of the length of the longer side of the rectangle.
2. For each candidate centre and radius, 50 discrete 7.2° arcs around the circle are tested.
3. At each point on the circumference of each arc, a pixel brightness is calculated using bilinear interpolation applied to the pixels in the image (since the points on the arc will not fall neatly on the image pixels). A pixel brightness is also interpolated at the same point in the same arc with a radius of 1 pixel less.
4. The difference between these yields a truly *directional* edge strength outwards from the centre of the arc. These strengths are summed over 12 points on each arc.
5. The 4 best arcs (those with the highest sum of edge strengths) between all tested circles at each of the 50 arc positions are used to build the final shape – i.e. 200 arcs in total, with varying radii and centre points.
6. Any outlying arcs whose radii are significantly above or below their local average are discarded.
7. The shape is drawn using a weighted moving average of radius and centre position, which smoothes the arcs into a coherent shape and approximates at weak areas where there is little or no evidence of edges. Arc strength (sum of edge strengths) is used as the weighting factor, so arcs with good evidence affect the shape more (Fig. 1).

The key points of this approach that allow it to deal with the problems listed above, are:

- The directional edge detection, accurate to the sub-pixel level, maximises the available contrast;
- The arc averaging aspect of the technique deals elegantly with damage and occlusion;
- The greatly reduced and geometrically constrained (arc-based) search regions minimise the effect of clutter.

It must be noted that this is a mapping function only: it requires as input an approximate centre point and size of the monument of interest.

---

<sup>1</sup> In image processing, the first step towards automatic object extraction is often the application of an edge-enhancement filter. This essentially determines how different pixels are from their neighbours: abrupt changes in brightness normally imply the edges of objects. The aim is to automati-

---

cally recognise objects in the scene, which are typically characterised by their edges.

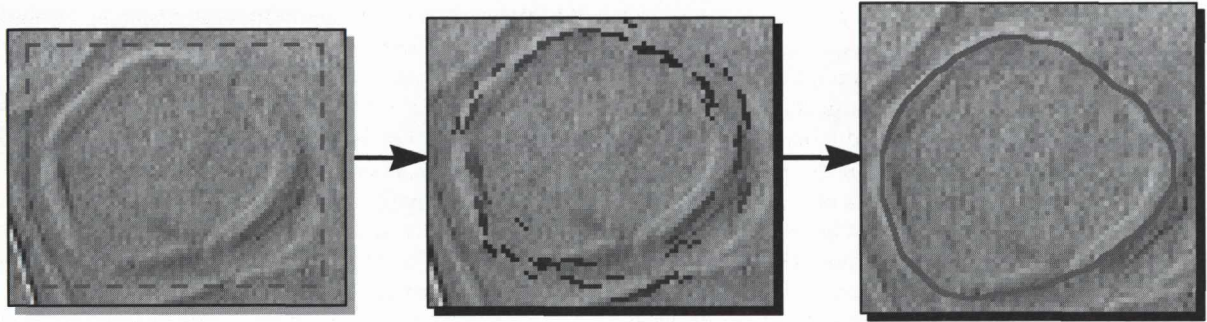


Fig. 1. Monument tracing. An area containing the feature of interest is identified. The computer then extracts arcs of varying strength, centre, and radius, rejects outliers, and smoothes the remaining arcs together using weighted moving averages into a coherent shape which is approximated at weak areas

The goal of automating not only monument mapping, but also detection, has proven to be very difficult. Some success has however been achieved through the application of a technique based on the Hough transform, which is able to produce the approximate location and size information required by the technique above. The major problem with this brute-force approach is the amount of processing time required, which currently runs to several hours per photograph.

## 2.2 Testing the Monument Mapping Technique

Since most object extraction techniques have been developed for optimality under specific conditions, it is difficult to objectively compare these techniques. Vernon suggests that quantitative though empirical assessments, carried out for specific problem domains, may be the best realistic means of comparison (Vernon 1991). A co-efficient of merit,  $R$ , suggested for this approach by Abdou and Pratt (1979) is defined as:

$$R = \frac{1}{\max(I_A, I_I)} \sum_{i=1}^{I_A} \frac{1}{1 + \alpha \cdot d^2} \quad (1)$$

where  $I_I$  and  $I_A$  represent the number of ideal and actual (detected) edge points,  $d$  is the separation distance of a detected edge point, normal to a line of ideal edge points, and  $\alpha$  is a scaling constant, typically 0.111, which can be adjusted to penalise edges offset from their true location. In order to assess the performance of object extraction approaches using a metric such as Abdou and Pratt's, it is necessary to know in advance the ideal position at which 'true' edges lie. In the case of archaeological monument extraction from aerial photographs this is impossible, since the 'true' edge-definition of monuments is often poor, and always highly subjective. For purposes of objective testing, therefore, a set of test images, representative of the problem domain, was developed.

A morphological study of monuments from aerial photographs of Bruff, Co. Limerick<sup>2</sup> was carried out, and a primary set of 4 shapes was then derived, in order to represent the morphological range encountered in sub-circular earthwork monuments<sup>3</sup>. In order to accurately simulate real data from the problem domain, a number of factors were considered:

- The majority of earthwork monuments in Ireland are situated in grasslands. An analysis of patches of grass scanned at different resolutions showed that typical grass 'noise' is Gaussian, and that there is no structure evident at different scales. All test images were assigned Gaussian noise with standard deviation equivalent to that typically found in Irish medium altitude aerial images.
- Since monuments are often damaged or occluded, a secondary set of shapes was derived from the first, with breaks in their boundaries.
- Many monuments – particularly those that are likely to be previously unknown – appear with very low tonal contrast to their surrounding (internal and external) environment. Each of the 8 shapes was therefore used to generate a set of images with varying contrast. The lowest contrast for each was set to 5%<sup>4</sup>.
- The presence of clutter produces strong edge responses in aerial images, some of which may be erroneously identified as archaeological monument boundaries. A set of scenes involving geometric clutter as well as objects of interest was therefore produced.

<sup>2</sup> The Bruff study involved a selection of the 200 aerial photographs taken for archaeological survey purposes on behalf of the Office of Public Works (OPW) and the Dept. of Archaeology, U.C.C. (see Doody 1993).

<sup>3</sup> The set of test shapes was designed to adhere to the ranges of quantitative morphological measurements such as circularity, rectangularity, and elongation.

<sup>4</sup> Given a 256-greyscale image, 5% contrast would imply that the shape of interest, representing a monument, would be rendered at about 13 greyscale values different from the background. This is significantly less than the random fluctuations in greyscale applied in order to simulate grass.

For the purposes of quantitative assessment, 5 object extraction operations (listed below) were applied to the test cases. In some cases, pre-processing and/or post-processing was required in addition to the operation being tested, in order to allow the operations to produce single-pixel width edge maps. The Abdou & Pratt performance metric presumes output of this type.

- **Marr-Hildreth:** The Marr-Hildreth operation (Marr and Hildreth 1980) was chosen as it is touted as an optimal derivative-based operator. It was followed by the following operations: threshold, thinning, and patch-size based noise suppression. See, for example, Castleman 1996 for a discussion of these and other image processing techniques.
- **Canny:** The Canny operation (Canny 1986) was applied with Gaussian smoothing. It was chosen due to its alleged optimal performance despite the presence of noise, and its single, accurately located response to a single edge.
- **Sobel:** The Sobel edge operator (see e.g. Castleman 1996) was chosen as it is broadly representative of the various derivative-estimation, direction invariant operations. It was preceded by Gaussian smoothing, and followed by thresholding, thinning, and patch-based noise suppression.
- **Hough:** The circle Hough transform (Hough 1962) was chosen due to its superior performance despite the presence of noise. It is more useful as an object detector rather than as a pixel-accurate shape extractor, if objects are of indeterminate shape. It is not therefore intended to compare the Hough transform as an edge extraction technique, but rather to assess its high level automatic detection performance.
- **AAS:** The performance of the sub-circular shape extraction algorithm, which has been described in this paper, is directly compared to the performance of the other techniques.

### 2.3 Contrast Tests

Contrast tests were applied using an ellipse shape (referred to as *ellipse\_1*). A perfect circle was not chosen

as this would be unrealistic and would give an unfair advantage to the AAS and Hough techniques. Figure 2 illustrates the performance of the operations under examination on the ellipse shape rendered at increasing contrasts.

Visually, it can be seen that the performance of the AAS technique degrades gradually at decreasing contrast, failing finally at about 9% contrast (Fig. 3). The other techniques all suffer dramatic performance degradation at 18% contrast and below: all have completely failed at contrast 12% (for example see figure 4).

### 2.4 Shape Tests

The four primary test shapes (*Circle*, *Ellipse\_1*, *Ellipse\_2*, *Rounded\_Rectangle*) were used to test the morphology-variant performance of the five operators. Each shape was tested at four different contrasts: two at the critical level identified by the preceding contrast tests (15% and 18%), and two at contrasts that did not prove to confuse any of the operators (37% and 92%). The average of the results over these four contrasts was used to determine the performance of an operator. The results are presented in figure 5. The Canny operation, as before, achieved the best results with the highest contrast images, but at other contrasts performed no better than the other standard operators. The Hough transform, not surprisingly, achieved perfect results with the *circle*, but performed badly on *ellipse\_1* and disastrously on the other 2 shapes.

The suitability of the 7.2° arc as a shape primitive is validated through this set of tests, which include shapes that are quite unlike circles. The performance of the technique described in this paper does however degrade as shapes become less and less circle-like. This is due to the fact that the arcs describing their edges are less well constrained by a tight range of radii and centre points, as well as the fact that the arc smoothing operation, while improving noise performance, distorts dissimilar neighbouring arcs.

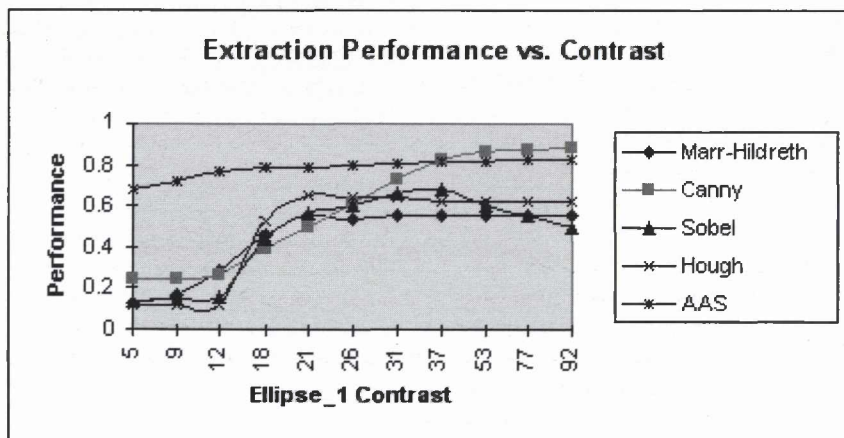


Fig. 2. Performances of the techniques under investigation on the ellipse\_1 shape. The X axis (contrast) is not a linear scale



Fig. 3. Gradual failure of the AAS monument tracing technique due to decreasing shape contrast. As edge evidence declines, the extracted shape tends towards a circle. (1) Ideal edge map, (2) result at contrast 21%, (3) result at contrast 18%, (4) result at contrast 12%, (5) result at contrast 9%



Fig. 4. Response of the Marr-Hildreth technique to decreasing contrast. (1) 21% contrast, (2) 18% contrast, (3) 12% contrast

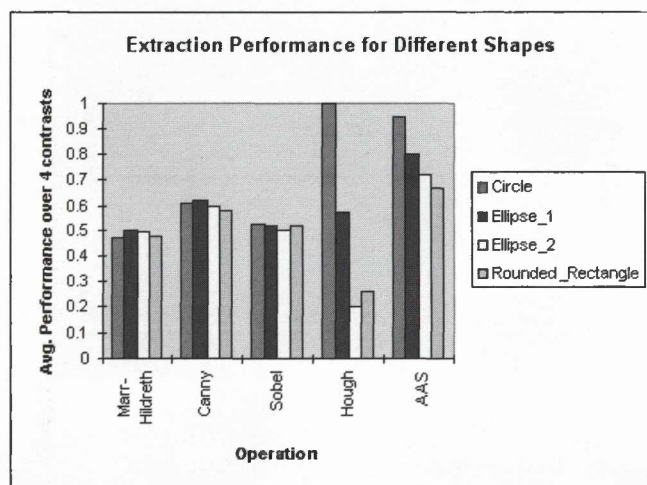


Fig. 5. Performances of the techniques under investigation on 4 different shapes. Each performance rating is an average of performance over 2 difficult (15%, 18%) and 2 easy (37%, 92%) contrasts

## 2.5 Damage Tests

In order to assess the performance of the operations when presented with damaged shapes, four shapes with increasingly large gaps in their boundaries were derived from the original test set. In each case, the Abdou & Pratt metric of an extracted shape was calculated against the full, undamaged version of the shape. Images at 92% contrast were used in each case. Figure 6 presents the absolute performances of the operations with these shapes.

The robustness of the Hough transform when searching for well-defined shapes (i.e. true circles) is evident. The AAS technique proved only marginally better than the Canny operation when operating on the damaged ellipses. The Marr-Hildreth, Canny, and Sobel operations all degraded by approximately the same per-

centage as each other on each damaged shape: this is not surprising, as these operations make no explicit attempt to estimate breaks in a boundary. Their performances simply represent the percentage of the object's boundaries that were presented to them. Figure 7 illustrates the results of the AAS operation on the two damaged ellipses. The breaks in the boundary of *ellipse\_1b* were not at critical places where the local arc radii or centre points were changing fast. However, the breaks in *ellipse\_2b*, particularly the break at the right-hand side of the shape, were larger and positioned at critical points. The estimation of weak arcs has visibly failed in this case, resulting in a relative performance of only 75% when compared to the operation's performance on an undamaged *ellipse\_2*.

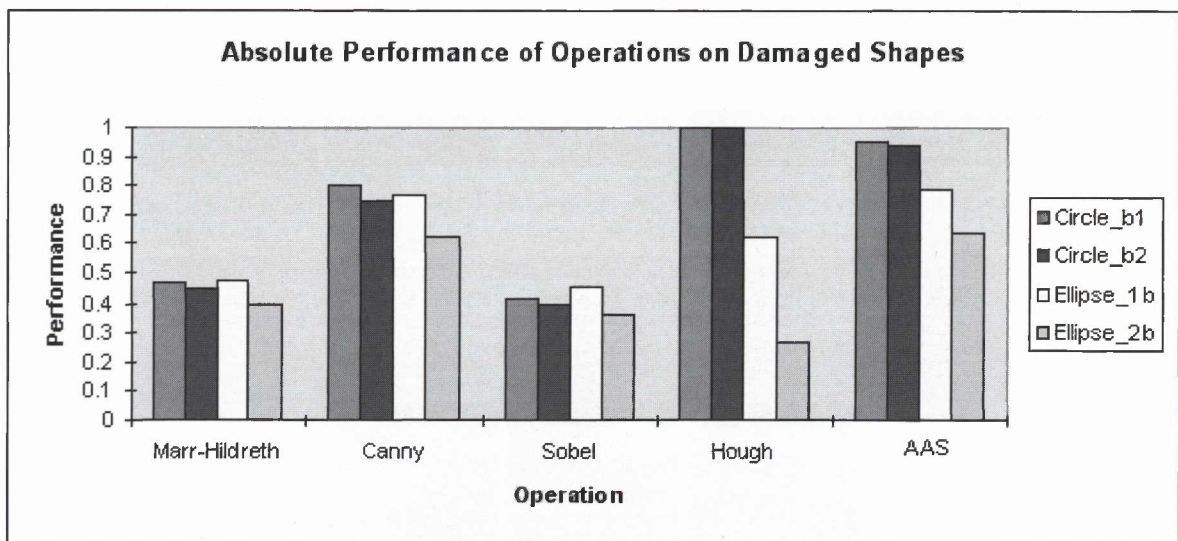


Fig. 6. Performances of the techniques under investigation on damaged shapes

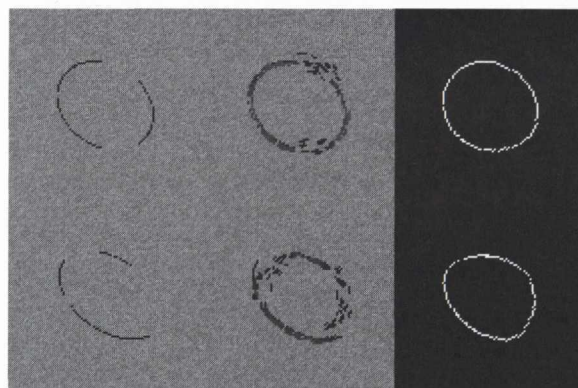


Fig. 7. Results of the AAS technique on ellipse\_1b and ellipse\_2b. (Top left) ellipse\_1b image at 92% contrast; (top middle) extracted arcs: the brighter arcs are those with higher strength coefficients; (top right) estimated shape; (bottom left) ellipse\_2b image at 92% contrast; (bottom middle) extracted arcs; (bottom right) estimated shape

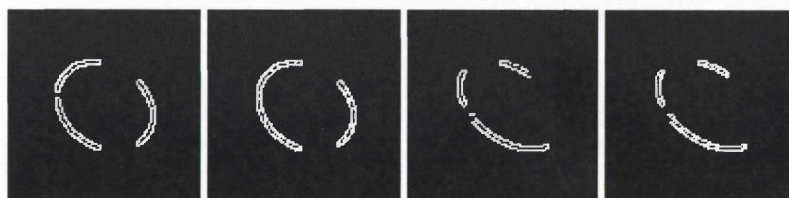


Fig. 8. Application of relaxation to damaged shapes. (1) Output of Canny on ellipse\_1b; (2) after relaxation; (3) output of canny on ellipse\_2b; (4) following relaxation

Since none of the standard operations under examination attempt to deal with broken boundaries, further tests were carried out by applying an image processing technique called 'relaxation', which is often used for this task (see Castleman 1996), to the results of the Canny operator. The gaps in the extracted boundary proved to be too large for the relaxation operation to fill. As illustrated by figure 8, only small insignificant breaks were fixed.

## 2.6 Clutter Tests

A final set of experiments was devised in order to estimate the performance of the operations on cluttered images. These tests were carried out on the *ellipse\_1* shape at 92% contrast. Figure 9 illustrates the relative performances of the operators, versus their own performance on uncluttered *ellipse\_1* images. It therefore presents the robustness of the techniques in the presence of clutter.

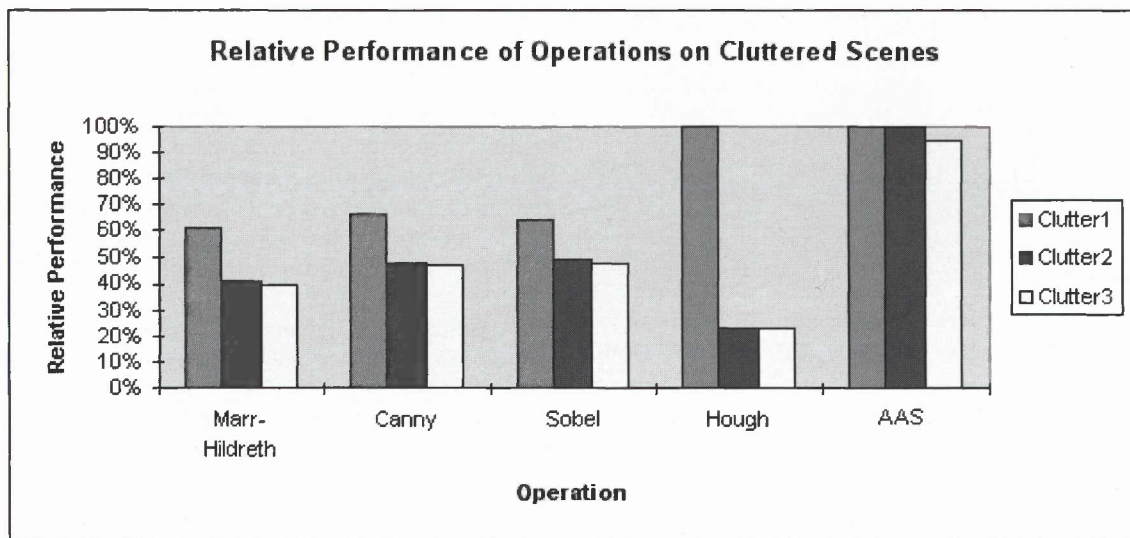


Fig. 9. Performances of the operations under investigation on cluttered ellipse\_1 images, relative to their own performances on the original ellipse\_1 image

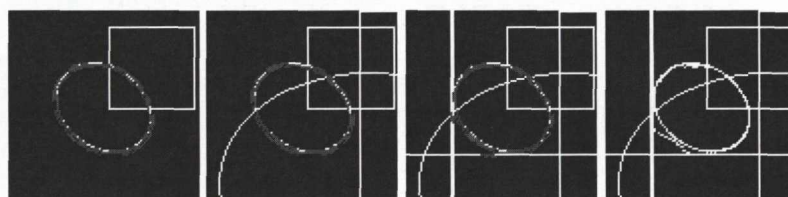


Fig. 10. Results of the AAS operation on cluttered scenes. (1) Arcs extracted from clutter\_1 image; (2) arcs extracted from clutter\_2 image; (3) Arcs extracted from clutter\_3 image; (4) Smoothed boundary extracted from clutter\_3 image

The AAS technique degraded in performance only with image *clutter\_3* (see figure 10). It is clear that this technique only degrades when clutter is present very close to the genuine edges. This further validates the aim of this approach to greatly cut down the edge search regions, to small, tightly-defined arc-shaped regions close to hypothesised object boundary pixels.

### 3 Digital Elevation Modelling

Given a stereo pair of photos, measurements can be made between corresponding points in the overlapping region, to determine the approximate height of these points. The measurements made are of the parallax apparent in the direction of flight of the plane – and can be made between any clearly distinguishable points in the photo overlap (Slama *et al.* 1980). This manual technique has been automated in the AAS. The software generates DEMs of small regions around individual monuments: it does not process the entire overlap between photographs because low-frequency distortions, due to such factors as camera tilt and paper shrinkage, render these larger DEMs inaccurate. It is beyond the scope of this paper to consider the DEM generation algorithm in detail: however, it was summarised in a previous CAA paper (Redfern 1999a), and is discussed in detail in Redfern *et al.* 1999.

A number of DEMs of monuments were generated by the AAS, and tested against Electronic Distance Measure (EDM)-derived DEMs of the same monuments. The monuments chosen represented a range of upstanding earthwork types, and their images also exhibited a range of textures and contrasts. Figure 11 provides one example, in which DEMs of Rathcroghan mound, Co. Roscommon, are presented. In this example, Pearson's correlation coefficient was calculated on a line-by-line (horizontal transept) basis, between the two DEMs. The average coefficient for these lines was 0.96. The heights of corresponding pixels in these DEMs were plotted against each other, and the slope of the regression line was calculated to be 0.92. For this 7m. monument, this could lead to a systematic error of 56 cm. (8%) when estimating the total height of the monument. Given that the standard deviation of errors (i.e. the uncertainty due to random errors) is 34 cm., the overall accuracy is to about 90 cm., which is less than 0.1% of the flying height above the landscape. It must be noted that this level of accuracy is only obtainable for small areas of the full overlap between photographs, in which low frequency geometric distortion is not a major issue. Indeed, it is interesting to note that the systematic errors in the test DEMs were found to be more severe in those monuments that covered larger ground areas.

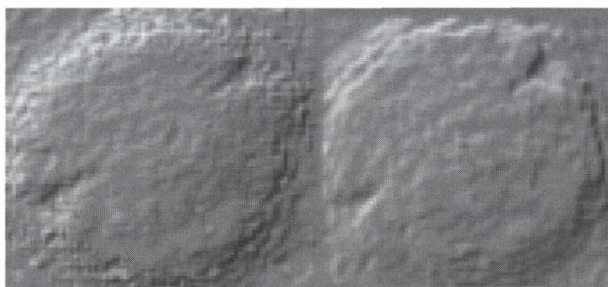


Fig. 11. DEMs of Rathcroghan mound, (left) generated by several weeks of ground survey, and (right) through use of the AAS

## 4 Classification

### 4.1 Morphological and Topographic Measurement

A variety of morphological and topographic metrics are considered to be significant to the classification of archaeological monuments, though some of these cannot be objectively collected because of the varying level of preservation of sites. This point is particularly relevant to initial survey from aerial photographs, since previously unknown sites are invariably those which survive as faint markings visible only from the air. Ground slope and aspect (facing) are important: ringforts, for example, tend to be on well-drained slopes. Size and overall shape are significant: it is suggested that larger, more accurately circular enclosures, for example, tend to be of prestigious ritual nature rather than domestic.

A number of other measurements, though considered significant to archaeological type designation, present problems in terms of objectivity. The compass direction of entrance(s) is important, though entrances are often hard to define, particularly from remote imagery, and it is often hard to tell if they are original.

and it is often hard to tell if they are original. Bank and ditch size (height, depth and width) are highly dependent on preservation. Measurements describing more complex structures (for example, systems of banks and ditches, or the nature of internal buildings) are notoriously difficult to collect, even from field survey, since neither structural changes that occurred during the period of occupation nor subsequent modifications of a site after its abandonment can be assessed (Barrett 1980).

A variety of spatial analyses between archaeological monuments and other environmental data are also relevant to site classification: for example nearest neighbour analysis, line-of-sight statistics, distance to nearest ecclesiastical site or to water. This type of analysis is however a higher level task in the domain of GIS, and is therefore beyond the scope of classification systems suitable for deployment as part of an early survey system. It is worth noting that *anything other than preliminary classifications* of archaeological sites cannot be attempted without a study of the wider landscape and inter-relationships between sites (Walker 1997).

The AAS classification scheme is based on a number of morphological and topographic measurements which are derived from a monument's extracted shape and from its DEM. These measurements, which are summarised in table 1, are those that (a) are deemed to be relevant to the morphological-topographic analysis of archaeological monuments, and (b) can be collected objectively from aerial photographs (Palmer 1976; Barrett 1980; Edis *et al.* 1989; Whimster 1989; Stout 1991). The DEM is used to derive slope and aspect information, through application of a 3-dimensional linear regression, i.e. determination of a best-fit plane (after Robinson 1981).

Table 1. The measurements made by the AAS software for monuments visible in vertical aerial photos

Measurement	Calculation	Notes
Circularity	(Area)/(Average distance of interior points from boundary) <sup>2</sup>	Maximised at 4π for a circle
Rectangularity	(Area)/(Area of minimum enclosing rectangle)	Maximised at 1.0 for a rectangle
Elongation	Length/Width	Length and width are calculated with respect to the principal axis of the shape
Total area	Pixels x area in photo of 1 pixel	The area represented by a single pixel in a photo is calculated automatically from user-supplied control points
Slope	Slope of best-fit plane	X,Y,Z ground co-ordinates of the points in the monument are submitted to a 3D linear regression
Aspect	Compass direction of best-fit plane	Orientation of photo/DEM is automatically calculated from user-supplied control points



#### 4.2 The development of the classification scheme

There are a number of requirements that should be met by an automated classification scheme of archaeological monuments, if it is to be applicable to wide-area assessment and regional or national database development:

- The scheme itself should be statistically significant. Archaeological significance cannot be ascertained in the short or medium term;
- Individual monument classifications should be reproducible. The wide range of monument preservation states therefore precludes incorporation of information such as entrances, and bank and ditch heights, widths and depths. While this in undoubtedly useful information, from a classification stance it is simply too subjective and affected by outside factors;
- The scheme should assist in the preliminary interpretation of monuments. It should therefore at least provide a data summary role, assisting the user to make sense of the sheer bulk of information.

In order to develop a typology of archaeological enclosures and sub-circular features visible in vertical aerial photographs, a set of 125 monuments were selected

from the Bruff Aerial Photographic Survey. The morphological and topographic measurements regarding each of these monuments, as outlined in table 1, were generated. In the case of the aspect (facing) measurement, the data were vectorised into a north component and an east component on the unit circle, since a simple angle is clearly not useful as it is not a continuous numerical measurement.

The data generated were normalised so that each variable fell within the range [0,1] (in order to ensure that all variables were of equal importance in the clustering process), and then submitted to agglomerative cluster analysis using Ward's method (see Everitt 1980), in order to objectively define typological groups. The resulting *dendrogram* is presented in figure 12: this is a tree of hierarchical relationships, which is used to graphically depict the clustering of data. One axis (in this case, the horizontal axis) plots the individual observations. The distances at which linkages are made between groups can be measured along the other axis: the more similar two observations or groups are, the closer to the origin of the vertical axis they are linked. Table 2 summarises the characteristic features of the 6 classes defined from the dendrogram.

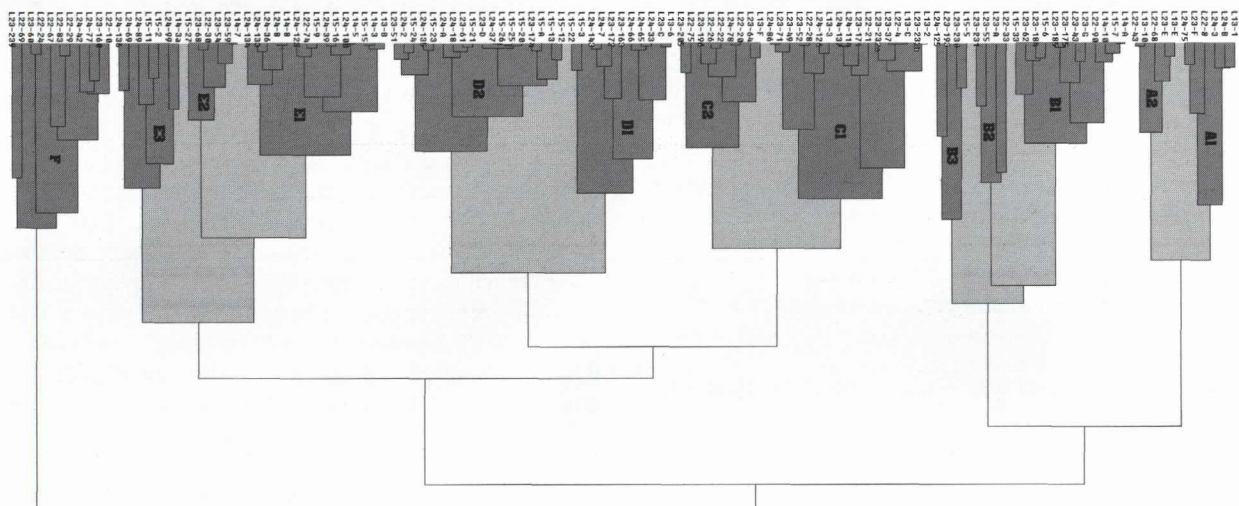


Fig. 12. Dendrogram resulting from cluster analysis of the 125 monuments from the Bruff survey. Monuments are presented along the top axis. The distances at which linkages are made from this top axis are inversely proportional to the strengths of those linkages, i.e. the similarity between the groups being linked. Resulting classes are shaded

Table 2. A summary of the 6 typological groups resulting from cluster analysis. 'Tightly defined' measures are those that unify a group (i.e. have low standard deviation) without actually being of unusually high or low mean value.

	No.	Radius	Circular.	Rectang.	Elong.	Slope	Facing
Group A	11	high	high	low	Low		
Group B	20					High	not N
Group C	26				tightly defined	Low	
Group D	29	low				tightly defined	N or NW
Group E	28						SE, E, or NE
Group F	11		low		High	Low	

### 4.3 Defence of the Classification Scheme

A coefficient,  $C$ , that measures 'tightness of clustering' was defined as follows:

$$C = \frac{\left( \frac{\sum D_g}{P_g} \right)}{\left( \frac{\sum D_a}{P_a} \right)} \quad (2)$$

where  $\sum D_g$  is the sum of Euclidean distances between each of the within-group pairs of objects,  $P_g$  is the number of within-group pairs of objects,  $\sum D_a$  is the sum of Euclidean distances between each pair of objects disregarding group membership, and  $P_a$  is the number of pairs of objects disregarding group membership. This coefficient measures the average ratio of the distance between objects in the same group, to the distance between objects disregarding grouping, and is minimised by a strongly clustered classification.

Monte-Carlo simulation was performed, in conjunction with the use of the  $C$  coefficient, in order to verify the statistical significance of the Bruff monument classification. In order to carry out this simulation, 500 sets of test measurements were generated, where each set comprised 125 'fake' monuments, whose measurements were selected randomly from correctly distributed data (the distribution of measurements for each variable was taken from that of the real Bruff data). Since radius and rectangularity were significantly correlated in the Bruff data (correlation coefficient -0.387), the rectangularity measurement of each 'fake' monument was adjusted as follows<sup>5</sup>:

$$rect_{new} = -0.387radius + rect_{old} \sqrt{1 - (-0.387)^2} \quad (3)$$

A similar adjustment was made to the elongation measurement of each "fake" monument, since in the Bruff data elongation was significantly correlated with circularity (correlation coefficient -0.456). The 500 sets of simulated data were submitted to cluster analyses, and  $C$  was calculated in each case. It was found that just 13 of the simulated sets produced stronger clustering than the real Bruff data. The AAS's classification may therefore be accepted at a 97.4% level of statistical significance.

It is obvious that there is a difference between statistical significance and archaeological significance. Statistical significance allows morphological and topographic observations to be made with some conviction; however, that is not to say that the factors causing these observations are necessarily archaeological -- "statistical significance is a necessary but not a sufficient condition for [archaeological] type designation." (Adams and Adams 1991: 177). Further archaeological research is

clearly required in order to determine the archaeological significance (if any) of the groups: a study carried out on the Rathcroghan/Carnfree complexes, in which data from the AAS was used in conjunction other data, has provided an initial assessment of this approach to classification. Aspects of this study are described in section 5. In the context of regional or national databases, which can often be difficult to query since they consist of subjective and descriptive entries made by many different archaeologists, a statistically significant and objective technique for monument classification has significant value, whether or not the classes have any direct archaeological meaning.

### 4.4 The Implementation of the classification scheme

Artificial Neural Networks (ANNs), which are essentially complex transfer functions based on simplified emulations of biological neural networks, have been well proven in the area of numerical classification, particularly in cases of 'noisy' data, where other classification approaches are more susceptible to error. They consist of one or more layers of nodes (artificial neurons). Numerical system inputs are received by an input layer of nodes, which operate on these values and output the results. The typical operation of a node involves a weighted summation of its inputs, and the application of a continuous non-linear function, in order to provide a bounded and differentiable output value.

The chosen ANN topology specifies connections between the nodes of the successive layers: the outputs resulting from the input layer become the input values to connected nodes in the other layers of the ANN, where further operations are performed. This feed-forward process continues until the outputs of the final layer, which represent the ANN's overall 'understanding' of the system inputs, are computed. The most widely proven ANN topology for pattern recognition tasks is the multi-layer perceptron (MLP): this specifies that the nodes in each layer are connected to *each* node in the preceding layer. It is common to use 3 layers of nodes in a MLP: the second layer, which has no connections to the 'outside world', is referred to as a *hidden layer*. It is this layer which adds sufficient internal complexity for complex patterns to be recognised.

In order to train a MLP to accurately match input values to target output values, the weights at each node are modified iteratively, most commonly through the 'back propagation' of errors from the output layer through the preceding layers (Rumelhart *et al.* 1985), which is essentially a credit-blame approach allowing the error attributed to each node to be used to modify the weights of its connected nodes.

In order to apply the developed monument typology as an automatic interpretation task in the AAS, a MLP approach was used. In designing the MLP architecture, i.e. the number of layers and the number of nodes in each layer, the fact that the end result was to represent discrete outputs was considered important. It would not be sensible, for example, to model the output from the network through a single node, even though this model

<sup>5</sup> The formula for generating correlated data was taken from: [http://www.uvm.edu/~dhowell/StatPages/More\\_Stuff/Gener\\_Correl\\_Numbers.html](http://www.uvm.edu/~dhowell/StatPages/More_Stuff/Gener_Correl_Numbers.html).

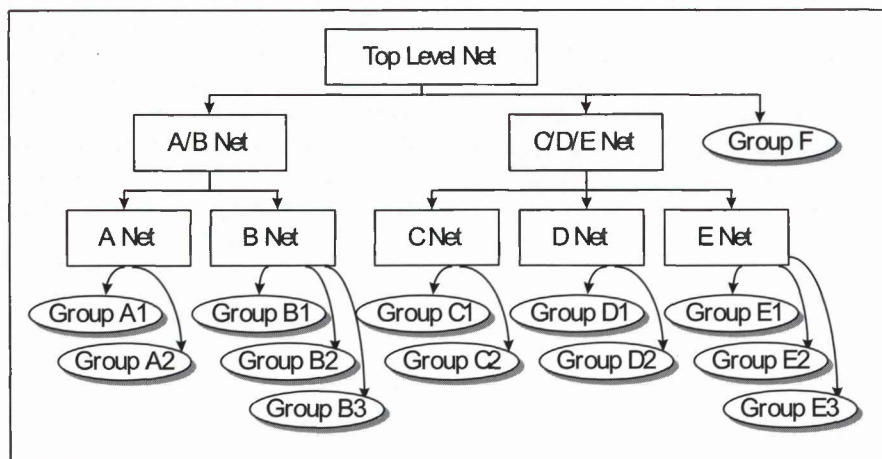


Fig. 13. The hierarchy of eight MLPs used to classify monuments. Rectangles represent neural networks, while ovals represent final classification decisions. Group F is sufficiently different from the other groups to be determined by the highest level network

was found to work well on the training and subsequent test data, since this implies a continuous output value. See Haykin 1994 for a general discussion of ANN architectures.

Various training experiments were carried out, and the final model, which proved to be highly reliable, involved a hierarchy of eight co-operating neural networks, as illustrated in figure 13. A hierarchical collection of MLPs is considered to be particularly suitable to the current classification task, since the groupings resulting from cluster analysis were inherently hierarchical in definition. The discrimination task to be trained for each network was derived directly from the classification dendrogram (figure 12). The top-level network, therefore, concentrates on separating monuments according to the three weakest linkages of the dendrogram, which distinguish (i) groups A and B, from (ii) groups C, D and E, from (iii) group F. On the second level of the hierarchy are two networks: the first separating group A from B, and the other separating group C from D from E. The bottom level of the hierarchy consists of a network for each of the groups A to E, which determine sub-group membership. Group F does not have any subgroups, and is identified by the top level network, since it is quite different to the other groups (the very last, i.e. least significant, linkage of the dendrogram is the one that joins group F to all of the others).

## 5 A Survey of Rathcroghan and Carnfree, Co. Roscommon, Ireland

A study encompassing a 20km x 20km region west of Strokestown, Co. Roscommon, was carried out using the AAS, employed in conjunction with a GIS containing information from the Sites and Monuments Record (SMR) and from NUI, Galway's ArchaeoGeophysical Imaging Project (AGIP) which ran from 1994-97 (see Waddell & Barton 1995). Near the centre of this region

are two distinct complexes of archaeological monuments: Rathcroghan and Carnfree.

Rathcroghan is a complex of monuments, situated about three miles northwest of the town of Tulsk, Co. Roscommon, and incorporates an impressive mound of some 5m height and 90m diameter. The ancient Celtic significance of the area is well known<sup>6</sup>, though its exact role(s) remain open to debate (see Waddell 1988) – some ritual purpose, probably royal inauguration and assembly, is presumed. The Carnfree complex is located on high ground some four miles to the south-southeast of Rathcroghan. This complex is named after its imposing burial cairn, which, as the royal inauguration site of the O'Conors in historical times, probably took over in function from Rathcroghan.

Over 800 monuments recorded in the SMR were extracted, and supplemented by 69 probable monuments newly discovered through the application of the AAS software. In order to determine which of these represented previously undiscovered monuments, the distance between each AAS-identified monument and each monument of relevant type in the SMR database was calculated<sup>7</sup>. The nearest monument extracted from the photographs, if any, within a 50m radius of each SMR monument was assumed to be the same monument. The remaining monuments were considered to be newly discovered<sup>8</sup>.

<sup>6</sup> Rathcroghan figures in the *Táin*, and is presumed to be the royal site of the Celtic kings of Connaught.

<sup>7</sup> Monuments considered relevant were those classified as ringforts, any types of enclosure, or any types of mound or barrow, since these are the types of monuments dealt with by the AAS.

<sup>8</sup> An analysis of the distance between AAS monuments and their nearest SMR monument showed 50m to be a suitably high distance to choose: the majority of AAS monuments were within 10m of an SMR monument, very few were between 10m and 40m from an SMR monument, while none were between 40m and 50m of one. It was also found that there was a strict one-to-one correspondence between AAS

Figure 14 illustrates, for the monuments represented in both the SMR and AAS databases, the correspondence between class designations. There appears to be an association between AAS class A and SMR 'ritual' monuments, and between AAS class D and 'domestic' monuments. This provides some tentative validation of the AAS classification scheme, though is perhaps best seen as a validation of the approach taken: more work is clearly required to refine the scheme itself. No AAS class appears to be associated with SMR enclosures: however, since the term 'enclosure' is somewhat ambiguous in that it may refer to both domestic and ritual monuments, this is perhaps not surprising.

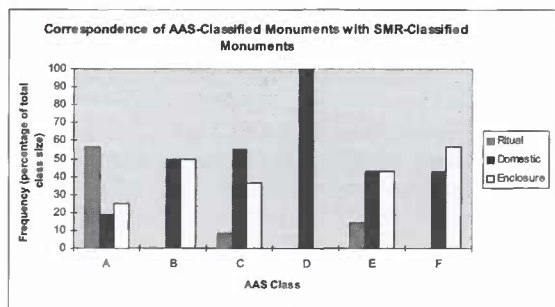


Fig. 14. Frequency histogram illustrating the correspondence between the AAS and SMR classification schemes in the Rathcroghan/Carnfree study

## 6 Conclusions

This paper has described efficient, objective means to assisting aspects of the work of the aerial archaeologist, as implemented in the Aerial Archaeology System (AAS) software. It has also described the testing and verification procedures that were carried out on the three related tasks of monument mapping, elevation modelling, and classification.

The monument tracing procedure has been shown to achieve better results, within its specific problem domain, than standard image processing techniques. There is still room for improvement of this procedure: for example, the weak-arc estimation technique could be improved through the use of centre and radius derivatives (rates-of-change) local to an arc, rather than through the simple weighted averaging process currently employed. The goal of fully automatic monument identification still remains unsolved: it is suggested that robust template-based techniques such as the Hough transform may provide part of the solution.

The accuracy of the AAS elevation modelling procedure over small areas of overlapping vertical aerial photographs has been validated. There are a number of ways in which this procedure could be improved; however, the scope of this paper does not allow a technical consideration of these issues. It should also be recognised that commercial software for topographic modelling from stereo pairs of photographs is becoming increasingly accessible for archaeological purposes.

and SMR monuments, i.e. AAS monuments were found to be close to *one and only one* SMR monument.

Though the statistical significance of the developed monument typology has been validated, the typology in its present state is essentially abstract, and therefore can represent only a first step towards archaeologically meaningful morphology-based classification. It is difficult to prove the objectivity of monument identification, i.e. to determine whether each mapped 'monument' does actually correspond to a genuine archaeological monument, or to something else, such as a small-scale geomorphological feature. Ideally, a field survey project would be used in order to provide the AAS with a set of unambiguous monuments and another set of unambiguous 'non-monuments', in order to provide information to train its ANNs to tell the difference. Field survey, selected excavation work, and further photographic surveys could also improve the abstract classification scheme and ascertain archaeological 'meaning' for its classes: the correspondence between known and AAS-derived monument classes in the Rathcroghan study indicates that such a strategy could work.

Startin (1992) describes the 'recording cycle' as a four stage process by which monuments are recorded in the British Sites and Monuments Record (BSMR). The first two stages are simple identification and basic descriptive recording, and the AAS represents a genuine improvement on existing techniques for carrying out these preliminary tasks. The BSMR suffers in particular from a lack of standardisation and thoroughness in the descriptive recording stage: many monuments indeed are only recorded at the simple identification stage of the recording cycle. The AAS provides the techniques for the basic morphological survey as well as the topographic survey of monuments, directly from aerial photographs. It therefore has the potential to speed up preliminary inspection and site measurement, and would most usefully be employed as an early part of hierarchical survey strategy.

## Acknowledgements

The author would like to thank John Waddell, Kevin Barton and Joseph Fenwick of the AGIP, NUI, Galway for the EDM data, and Martin Doody of the Discovery Programme, Dublin, for photographs and supporting documentation from the Bruff survey.

## References

- Abdou, I.E. and Pratt, W.K. 1979. Quantitative Design and Evaluation of Enhancement/ Thresholding Edge Detectors, *Proceedings of IEEE* 67, 753-63.
- Adams, Y.A. and Adams, E.W. 1991. *Archaeological Typology and Practical Reality*. Cambridge: Cambridge University Press.
- Barrett, G.F. 1980. A Field Survey and Morphological Study of Ring-Forts in Southern County Donegal, *Ulster Journal of Archaeology* 43, 39-51.
- Canny, J.F. 1986. A Computational Approach to Edge Detection, *IEEE Transactions on Pattern Analysis and Machine Intelligence* 8, 679-98.
- Castleman, K. 1996. *Digital Image Processing*. Prentice Hall, NJ, USA.

- Crawford, O.G.S. 1929. *Air Photography for Archaeologists, Ordnance Survey Professional Papers 12*, London.
- Darvill, T. 1996. *Prehistoric Britain From the Air: A Study of Space, Time and Society*. Cambridge: Cambridge University Press.
- Doody, M.G. 1993. The Bruff Aerial Photographic Survey, *Tipperary Historical Journal*, 173-80.
- Edis, J., MacLeod, D. and Bewley, R. 1989. An Archaeologist's Guide to Classification of Cropmarks and Soilmarks, *Antiquity* 63, 112-126.
- Everitt, B. 1980. *Cluster Analysis*. 2<sup>nd</sup> edn. London: Heinemann Educational Books.
- Haigh, J.G.B., Kisch, B.K. and Jones, M.U. 1983. Computer Plot and Excavated Reality. In: G.S. Maxwell (ed), *The Impact of Aerial Reconnaissance on Archaeology*, 85-91, The Council for British Archaeology, London.
- Hampton, J.N. 1983. Some Aspects of Interpretation and Mapping of Archaeological Evidence from Air Photography. In: G.S. Maxwell, (ed), *The Impact of Aerial Reconnaissance on Archaeology*, 109-123, Council for British Archaeology Research Report 49, London. 109-123
- Haykin, S. 1994. *Neural Networks: A Comprehensive Foundation*. New York: Macmillan.
- Hingley, R. 1991. The Purpose of Crop Mark Analysis, *AARGnews* 2, 38-43.
- Hough, P.V.C. 1962. A Method and Means for Recognising Complex Patterns. *U.S. Patent No. 3069654*.
- Lemmens, J.P.M., Stancic, Z. and Verwaal, R. 1993. Automated Archaeological Feature Extraction from Digital Aerial Photographs. In: J. Andresen, T. Madsen and I. Scollar (eds), *CAA92 - Computing the Past: Computer Applications and Quantitative Methods in Archaeology*, 45-51, Aarhus University Press, Aarhus.
- Marr, D. and Hildreth, E. 1980. Theory of Edge Detection, *Proceedings of the Royal Society London* 207, 187-217.
- Palmer, R. 1976. Interrupted Ditch Enclosures in Britain: The Use of Aerial Photography for Comparative Studies, *Proceedings of the Prehistory Society* 42, 161-86.
- Palmer, R. 1991. Approaches to Classification, *AARGnews* 2, 32-37.
- Redfern, S. 1997. Computer Assisted Classification from Aerial Photographs, *AARGnews* 14, 33-38.
- Redfern, S., Lyons, G. and Redfern, R.M. 1998. The Automatic Morphological Description and Classification of Archaeological Monuments from Vertical Aerial Photographs, *Proceedings of OEMI/IMVIP Joint Conference*, 300-315, Maynooth, Ireland.
- Redfern, S. 1999a. A PC-Based System for Computer Assisted Archaeological Interpretation of Aerial Photographs. In: L. Dingwall, S. Exon, V. Gaffney, S. Laflin and M. van Leusen (eds), *CAA97 - Archaeology in the Age of the Internet: Computer Applications and Quantitative Methods in Archaeology*. BAR International Series 750. Abstract p. 162, entire paper on the volume's CD ROM.
- Redfern, S. 1999b. A Framework for Digital Wide-Area Survey from Aerial Photographs, with Application to Rathcroghan and Carnfree, Co. Roscommon. Submitted to *Journal of Irish Archaeology*.
- Redfern, S., Lyons, G. and Redfern, R.M. 1999. Digital Elevation Modelling of Individual Monuments from Aerial Photographs. Submitted to *Archaeological Prospection*.
- Riley, D.N. 1987. *Air Photography and Archaeology*. London: Duckworth.
- Robinson, E.A.. 1981. *Least Squares Regression in Terms of Linear Algebra*. Dordrecht (Holland): Reidel.
- Rumelhart, D.E., Hinton, G.E. and Williams, R.J. 1985. Learning Internal Representations by Error Propagation, *ICS Report 8506*. Institute for Cognitive Psychology, Univ. of California.
- Scollar, I. et al. 1990. *Archaeological Prospecting and Remote Sensing*. Cambridge: Cambridge University Press.
- Slama, C., Theurer, C. and Henriksen, S. (eds) 1980. *Manual of Photogrammetry*, 4th edition. American Society of Photogrammetry, Va.
- Startin, B. 1992. The Monuments Protection Programme: Archaeological Records. In: C.U. Larsen (ed.), *Sites & Monuments: National Archaeological Records*, 201-206, National Museum of Denmark, Copenhagen.
- Stout, M. 1991. Ringforts in the South-West Midlands of Ireland, *Proceedings of the Royal Irish Academy* 91, 201-241.
- Vernon, D. 1991. *Machine Vision*. New York: Prentice Hall.
- Waddell, J. 1988. Rathcroghan in Connacht, *Emania* 5, 5-18.
- Waddell, J. and Barton, K. 1995. Seeing Beneath Rathcroghan, *Archaeology Ireland* 9, 38-41.
- Walker, S.D. 1997. Who's Afraid of Morphological Analysis? *AARGnews* 14, 27-32.
- Whimster, R. 1989. *The Emerging Past: Air Photography and the Buried Landscape*. Royal Commission on the Historical Monuments of England, London.